ACADEMIC PRESS

Available online at www.sciencedirect.com

SCIENCE DIRECT®

Journal of Magnetic Resonance 164 (2003) 136–144

JMR Journal of Magnetic Resonance

www.elsevier.com/locate/jmr

Regularized resolvent transform for direct calculation of 45° projections of 2D *J* spectra

Geoffrey S. Armstrong, Jianhan Chen, Kristin E. Cano, A.J. Shaka, and Vladimir A. Mandelshtam*

Department of Chemistry, University of California, Irvine, CA 92697-2025, USA

Received 7 March 2003; revised 8 March 2003

Abstract

The regularized resolvent transform (RRT) has been applied in a novel way to *J*-resolved spectra. This involves the direct calculation of the 45° projection without constructing the 2D spectrum. The results show a significant resolution enhancement over that obtained by the 45° projection of a 2D Fourier spectrum, even for much larger signals. In particular, RRT is able to resolve peaks that belong to different overlapping multiplets in a very crowded spectral region, where the conventional technique fails for any signal size. The resolving power of this method along with the significantly shorter signals required, make this method a powerful tool in spectral assignment.

Keywords: Spectral estimation; Resolution enhancement; Regularized resolvent transform; Filter diagonalization method; 2D *J* spectrum

1. Introduction

While coupled proton spectra contain a lot of information, in very crowded spectra the couplings can often hamper attempts to assign structure. It would thus be desirable to obtain a proton spectrum with the couplings removed, showing only singlets for each distinct proton. One technique to obtain this has been the projection along the 45° axis of a *J*-resolved 2D spectrum [1]. Unfortunately, due to phase-twist lineshape [2] in the 2D spectrum, the resolution of the resulting projection has suffered. Methods have been proposed to combat this problem, such as pseudo-echo filtering [3], or sine-bell weighting of the signal [4], but these methods degrade the sensitivity of the 2D spectrum, distort intensities, and often do not offer a significant enhancement to the projection. In this paper we apply the regularized resolvent transform (RRT) to a 2D *J*-resolved data set in a novel way to obtain a high-resolution proton decoupled spectrum without calculating a projection from a 2D spectrum. The 1D projection is calculated directly from the data to yield singlets that are not hampered by the phase-twist lineshape.

RRT is a linear algebraic technique for high resolution spectral analysis of multidimensional NMR data. It was introduced recently [5] as an extension of the filter diagonalization method (FDM) [6–11] (also see the review [12]). The main difference between the two methods is that the RRT is a *spectral estimator*, i.e., it constructs the spectrum without calculating the spectral parameters, while FDM essentially constructs the *line list* prior to the spectral estimation. In principle FDM provides more information but is also more demanding than RRT. RRT deals with ill-conditioned linear systems, a very well studied problem (see, e.g., the tutorial [13]), while FDM deals with ill-conditioned generalized eigenvalue problems, a more difficult problem (a package to solve ill-conditioned generalized eigenvalue problems named GUPTRI [14] exists, but we have not had success in applying it to FDM). Unlike most other linear algebraic approaches, both methods are truly multidimensional (i.e., are not reduced to processing 1D slices of multidimensional data) and do not involve large

* Corresponding author. Fax: 1-949-824-8571.
E-mail address: mandelsh@uci.edu (V.A. Mandelshtam).

1090-7807/$ - see front matter © 2003 Elsevier Science (USA). All rights reserved.
doi:10.1016/S1090-7807(03)00129-0

matrices even when the data size is large. In both FDM and RRT, the linear algebraic problems are solved in small Fourier subspaces corresponding to small windows in the frequency domain.

The usefulness of FDM has already been demonstrated for the calculation of double absorption spectra of purely phase modulated 2D data [8,9] or the direct calculation of absorption mode 45° projections of the 2D *J* spectra, in which the proton multiplets are collapsed into singlets [15]. The latter idea led to an interesting generalization to the case of two new experiments, the singlet-HSQC and singlet-TOCSY [16], which are, respectively, 3D and 4D experiments. In these experiments, one *J* dimension for 2D HSQC and two *J* dimensions for 2D TOCSY are added to the conventional experiments, followed by construction of 2D 45° projections, and resulting in the 2D absorption-mode spectra with singlets in place of the original multiplets. In the latter applications, just 2 points along each *J* dimension were used, thus effectively employing only a few 2D data sets. In other words, in these 3D and 4D experiments the experimental time was similar to that of the conventional 2D experiments. However, these applications also revealed some problems, associated mainly with the fact that the spectral widths in the *J* dimensions are by about two orders of magnitude greater than that of the proton chemical shift dimension. The 45° direction then corresponds to $\sim 10^2$ points in the proton dimension and one point in the *J* dimension. In [9,15,16] the construction of effective projected Hamiltonian(s) that are then diagonalized to yield the ultimate 45° projections required the solution of an additional ill-posed linear algebraic problem. This led to instabilities in the spectra. In [9,15], in order to get rid of the artifacts, regularization was carried out by extensive signal averaging, while in [16] *pseudo-noise averaging* was implemented. Both regularization approaches require multiple applications of FDM and so result in a substantial increase of the cpu-time. An alternative to the FDM averaging procedure, named FDM2K, to regularize the spectra was also proposed [11]. Generally, FDM2K works well, while requiring minimal computational effort, but its use for calculating 45° projections may still require some work because of the need to solve and, therefore, regularize, at least two consecutive ill-posed generalized eigenvalue problems. The regularization in RRT is more robust than in FDM2K giving a more reliable result, while it is also controlled by the regularization parameter *q*: larger values of *q* lead to stronger artifact suppression and more uniform spectral estimates but sacrifice the resolution. By integrating out the *J*-dimension one can obtain a pseudo-absorption 45° projection. This method would avoid the tricky scaling problem, but would lose the advantage of a *direct method*. Moreover, the integration must be done on a very fine frequency grid, which may not be a problem in the 2D case, but it becomes a numerical bottleneck in 3D and 4D experiments where *J* projections are of interest [16].

Dissatisfaction with the previous methods provoked an extensive search for a new method that is direct, fast, and avoids the subtle scaling procedure, and led us to the approach described in this paper. We interpolate the signal on a new grid with the same sampling rate in the two dimensions and then apply RRT to the new resampled data to directly and efficiently compute a 45° projection. The only drawback to this method is that the intensities in the 45° projection are not quantitative, in most cases.

2. Theory

2.1. Spectral representations of 2D J time signals

Consider a general complex valued 2D time signal $c(t,\tilde{t})$ with $t = n\tau$ $(n = 0,\ldots,N-1)$ and $\tilde{t} = \tilde{n}\tilde{\tau}$ $(\tilde{n} = 0,\ldots,\tilde{N}-1)$ defined on an equidistant rectangular time grid of size $N_{\text{total}} = N \times \tilde{N}$. We use a convention in which *t* corresponds to the acquisition time dimension. By "tilde," as in $\tilde{t}$, we define the variables associated with the *J* dimension. Generally the sampling rate ratio $\tilde{\tau}/\tau$ is a large number, of the order of 100, which is practically justified by the small spectral width in the *J*-dimension of the order of 100 Hz; *N* is of the order of 10^3–10^5 and $\tilde{N}$ small (e.g., $\tilde{N} = 16$ and usually does not exceed 128).

For a noiseless case we assume that the 2D data is well represented by the form

$$c(t,\tilde{t}) = \sum_{k=1}^{K} d_k \mathrm{e}^{-\mathrm{i}t\omega_k} \mathrm{e}^{-\mathrm{i}\tilde{t}\tilde{\omega}_k} \tag{1}$$

with the complex frequencies ω_k and $\tilde{\omega}_k$ and amplitudes d_k characterizing the *K* spectral features in the 2D frequency domain. For simplicity, the signal is assumed to be phased, i.e., the amplitudes d_k are assumed to be real. The real part of a complex frequency defines the position of the corresponding resonance and the imaginary part, its width. Usually, one assumes that the signal decays when $t \to \infty$ and $\tilde{t} \to \infty$, which implies that all the imaginary values are negative, however, this constraint may cause numerical and even conceptual problems and will be implemented only in some special cases. For noisy data the same model is used, however *K* is no longer well defined, as it is now used to represent both the true peaks and noise; the noise amplitudes are allowed to be complex-valued and the noise frequencies may have positive imaginary parts. Fortunately, in the present framework *K* does not have to be an adjusting parameter, e.g., we do not need to assume any particular value for it. This avoids many potential difficulties, often

present in other approaches designed to solve the harmonic inversion problem. The assumption (1) with some fixed K is only used as a reference and for derivations.

For demonstration purposes we generated a model 2D J signal using a predefined set of spectral parameters $\{\omega_k, \tilde{\omega}_k, d_k\}$ $(k = 1, \ldots, K)$ resembling the aromatic region of the proton spectrum of phenanthridinone. In Fig. 1 (top) we show a 1D proton spectrum obtained by Fourier transformation of the first increment of the signal

$$I(\omega) = \int_0^\infty \mathrm{d}t c(t,0)\mathrm{e}^{\mathrm{i}\omega t}. \tag{2}$$

From now on we will use the convention in which the 1D absorption spectrum is defined by

$$A(\omega) := \mathrm{Re}\{I(\omega)\}, \tag{3}$$

which assumes all amplitudes d_k to be real. Clearly, if the model (1) holds, $I(\omega)$ can also be represented in terms of the spectral parameters

$$I(\omega) = \mathrm{i}\sum_k \frac{d_k}{\omega - \omega_k}. \tag{4}$$

An ideal 2D J spectrum (particularly, no strong coupling artifacts) corresponds to all proton multiplets aligned along the 45° direction in the 2D frequency domain as shown in Fig. 1 (middle). In this idealized case the corresponding 45° projection will consist of singlets for each multiplet as shown in Fig. 1 (bottom). The 2D spectrum in Fig. 1 was constructed using the double-absorption expression in terms of the spectral parameters:

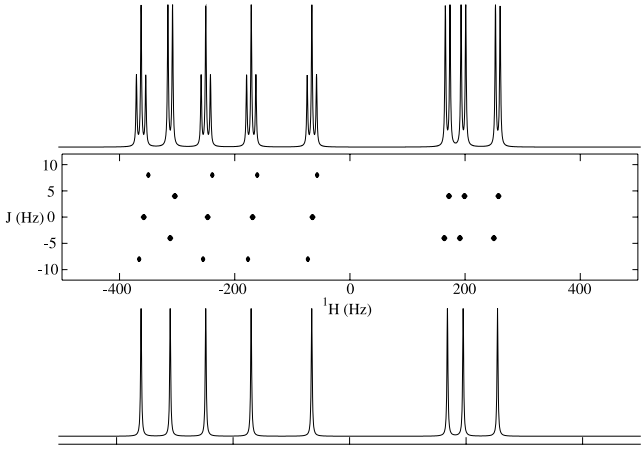

Fig. 1. The three spectra are constructed from a list of frequencies corresponding to the aromatic region of phenanthridinone. The top spectrum is the Fourier transformation of the first increment of a 2D J model signal constructed from the line list. The spectrum in the middle is the ideal 2D J spectrum obtained if a double absorption spectrum could be obtained. The bottom spectrum is the theoretical projection obtained from this "double-absorption" 2D J spectrum.

$$A_{2\mathrm{D}}(\omega, \tilde{\omega}) = \sum_k \mathrm{Im}\left\{\frac{d_k}{\omega - \omega_k}\right\}\mathrm{Im}\left\{\frac{1}{\tilde{\omega} - \tilde{\omega}_k}\right\}. \tag{5}$$

By analogy with Eqs. (3) and (4) an absorption mode projection is given by $A_p(\omega) := \mathrm{Re}\{I_p(\omega)\}$ with

$$I_p(\omega) = \mathrm{i}\sum_k \frac{d_k}{\omega - \omega_k + \tilde{\omega}_k}. \tag{6}$$

Note though that in theory for each peak the two line widths are the same and, therefore, the difference $\mathrm{Im}\{\omega_k - \tilde{\omega}_k\} = 0$. This implies that the directly computed projection $A_p(\omega)$ will consist of δ-peaks centered at frequencies $\omega = \mathrm{Re}\{\omega_k - \tilde{\omega}_k\}$, thus potentially leading to arbitrarily high resolution. (Note, that the finite widths of the peaks in a 2D spectrum give finite widths of the singlets in the projection, when the latter is obtained by integration of the 2D spectrum.) However, due to either experimental imperfections or numerical errors $\mathrm{Im}\{\omega_k - \tilde{\omega}_k\}$ is never exactly zero and, more importantly, has an arbitrary sign, which for a positive d_k defines whether the corresponding peak will be pointing up or down if Eq. (6) is used. One way to remove this ambiguity is to consider the quantity $A_p(\omega + \mathrm{i}\Gamma)$, which will turn each δ-peak to a Lorentzian with positive width Γ. Practically, for a sufficiently large smoothing parameter Γ this procedure will flip all the negative signs to positive. However, as will be discussed later this procedure may still cause artifacts.

Unlike the conventional 1D absorption spectrum, neither $A_{2\mathrm{D}}(\omega, \tilde{\omega})$ nor $A_p(\omega)$ can be computed or even estimated by conventional means, that is, by Fourier transformation of the purely phase modulated time domain data $c(t, \tilde{t})$. For instance, even though Eq. (6) is formally represented by the Fourier integral of the data,

$$I_p(\omega) = \int_0^\infty \mathrm{d}t c(t,-t)\mathrm{e}^{\mathrm{i}t\omega}, \tag{7}$$

the integration has to be performed along the line in the 2D time domain that is not available experimentally. As such in the FT framework one would usually utilize the absolute value spectrum. In order to enhance the resolution (compromised by not using the absorption mode spectrum, with its large dispersion mode wings) one can implement heavy apodization functions (e.g., a sine-bell $g(t) = \sin(\pi t/T)$) [4]:

$$I_{2\mathrm{D}}(\omega, \tilde{\omega}) = \int_0^T \mathrm{d}t \int_0^{\tilde{T}} \mathrm{d}\tilde{t}\; c(t,\tilde{t})\mathrm{e}^{\mathrm{i}\omega t}\mathrm{e}^{\mathrm{i}\tilde{\omega}\tilde{t}} g(t)\tilde{g}(\tilde{t}). \tag{8}$$

A 45° projection of $|I_{2\mathrm{D}}(\omega, \tilde{\omega})|$ can now be obtained by tilting it and then integrating over $\tilde{\omega}$:

$$F_p(\omega) = \int \mathrm{d}\tilde{\omega}|I_{2\mathrm{D}}(\omega - \tilde{\omega}, \tilde{\omega})|. \tag{9}$$

The corresponding 2D FT spectrum and the projected spectrum are shown in Fig. 2 for a typical 2D data set. Apparently, the singlets in the projected spectrum in

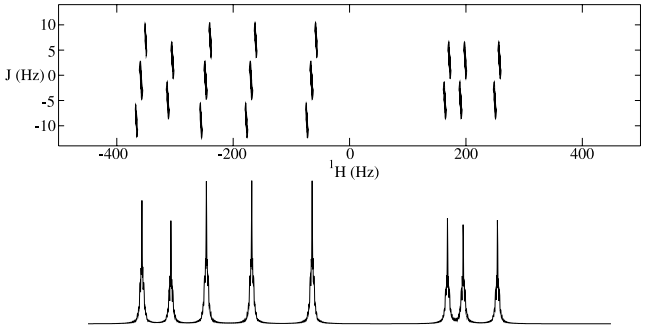

Fig. 2. The two spectra in this figure were obtained from a model 2D J signal constructed to represent the aromatic region of phenanthridinone (as in Fig. 1). The top spectrum is the 2D FT of the signal, weighted with a sine-bell function. The bottom spectrum is obtained by integrating the 2D spectrum along the 45° direction.

Fig. 2 are not significantly sharper than the original proton multiplets (Fig. 1, top). Clearly, this procedure leads to inferior resolution compared to that of the true 2D absorption spectrum or its projection, even when the data is available over a large region in the 2D time domain. In the present paper we discuss various methods to compute $A_p(\omega)$ or its analogues and present an efficient and direct method based on RRT.

2.2. Signal resampling

For the reason mentioned above we wish to deal with a 2D J signal that is sampled at the same rate in the two time dimensions. At first glance this problem may seem unimportant and, in our original papers on the subject, its importance was not recognized. Indeed, it is irrelevant in the framework of the Fourier spectral analysis, while its efficient and correct solution turns out to be crucial for the RRT to become operationally easy to implement. (Note again that in [9,15,16] the problem of having different sampling rates occurred at a different stage and its solution required a nontrivial numerical procedure.)

There are two obvious ways to make the two time steps the same. One is to make them both equal to $\tilde{\tau}$. While easy to implement, this will obviously lead to folding artifacts. The other way is to reconstruct the data on the new time grid with the same time step equal to τ by interpolating the slowly-varying original data in the J-dimension

$$y_{nm} := c(n\tau, m\tau) \quad (n = 0, \ldots, N-1,\ m = 0, \ldots, M-1)$$

with $M = (\tilde{N}-1)\tilde{\tau}/\tau + 1$. This procedure is justified because the signal-to-noise ratio (SNR) in 2D J experiments is usually high and the time evolution along the J-dimension is slow (small coupling frequency). Ideally, one could use true 2D interpolation or approximation schemes. The effect of using sophisticated schemes is unknown and will be explored in the future. Here we implement the most primitive, 1D cubic spline interpolation [17], which seems to suffice for our purposes. In practice, one should ensure that the data being interpolated behaves well, and has no spurious points, otherwise slight problems could be amplified by the interpolation routine.

We can now rewrite the assumption (1) for the resampled data in a more convenient form

$$y_{nm} = \sum_{k=1}^{K} \mathrm{d}_k (u_k)^n (\tilde{u}_k)^m \tag{10}$$

with $u_k := \mathrm{e}^{-\mathrm{i}\tau\omega_k}$ and $\tilde{u}_k := \mathrm{e}^{-\mathrm{i}\tau\tilde{\omega}_k}$.

For discretely sampled data as in Eq. (10) it is more appropriate to replace the spectral representations (3)–(6) arising from the Fourier integrals by that corresponding to the discrete Fourier sums (see the discussion in [12]). In particular, Eq. (3) is replaced by

$$I(\omega) = \sum_k \frac{\tau d_k}{1 - u_k/z} \tag{11}$$

with $z := \mathrm{e}^{-\mathrm{i}\tau\omega}$ and the 45° projection (6) is replaced by

$$I_p(\omega) = \tau \sum_k \frac{d_k}{1 - u_k/(z\tilde{u}_k)}. \tag{12}$$

Note that Eq. (12) is essentially equivalent to Eq. (6) as long as $\mathrm{Im}\{\omega_k - \tilde{\omega}_k - \omega\} \ll (2\pi/\tau)$ or equivalently $|u_k/(z\tilde{u}_k)| \approx 1$. Here, the real part of Eq. (12), $A_p(\omega + \mathrm{i}\Gamma) := \mathrm{Re}\{I_p(\omega + \mathrm{i}\Gamma)\}$, gives the true absorption spectrum. However, we have found that the pseudo-absorption spectrum $A_p^{(2)}(\omega) := |I_p^{(2)}(\omega)|$ with

$$I_p^{(2)}(\omega) := \tau^2 \sum_k \frac{d_k}{(z\tilde{u}_k - u_k)^2} \tag{13}$$

numerically behaves much better and, in particular, is free from the drawbacks arising from the intrinsically small widths. Unfortunately, $|I_p^{(2)}(\omega)|$ is different from the absorption spectrum: the amplitudes d_k are not squared, but the peak amplitudes in Eq. (13) are scaled by the factor equal to $\mathrm{Im}\{\omega_k - \tilde{\omega}_k - \omega\}$ (see the discussion in [12]). So narrow peaks in the pseudo-absorption spectrum will often be overemphasized in $|I_p^{(2)}(\omega)|$.

2.3. Regularized resolvent transform

2.3.1. Noiseless case

First, assume that the data y_{nm} satisfies the form of (10) exactly. Consider two diagonalizable commuting complex symmetric $K \times K$ matrices U and $\tilde{U}$ with the complex poles u_k and $\tilde{u}_k$ being their eigenvalues:

$$U = \sum_{k=1}^{K} u_k \Upsilon_k \Upsilon_k^{\mathrm{T}}; \quad \tilde{U} = \sum_{k=1}^{K} \tilde{u}_k \Upsilon_k \Upsilon_k^{\mathrm{T}}. \tag{14}$$

Given a column vector Φ satisfying

$$d_k = \left(\Phi^{\mathrm{T}} \Upsilon_k\right)^2, \tag{15}$$

the assumption (10) can now be rewritten in an equivalent form [7,6,9]

$$y_{nm} = \Phi^{\mathrm{T}} U^n \tilde{U}^m \Phi. \tag{16}$$

Furthermore, using the definitions of U, $\tilde{U}$, and Φ (Eqs. (14) and (15)) we can rewrite the spectra (12) and (13) as:

$$I_p(\omega) = z\tau \Phi^{\mathrm{T}} (z\tilde{U} - U)^{-1} \tilde{U} \Phi, \tag{17}$$

$$I_p^{(2)}(\omega) = \tau^2 \Phi^{\mathrm{T}} (z\tilde{U} - U)^{-2} \Phi. \tag{18}$$

The evaluation of Eqs. (17) and (18) can be done using exclusively the available data y_{nm} through the relationship (16) without the explicit knowledge of the auxillary objects U, $\tilde{U}$, and Φ. The needed matrix elements are expressed in a Fourier subspace representing a particular a priori chosen small spectral window $[\omega_{\min}, \omega_{\max}]$ in the proton chemical shift dimension,

$$\omega_{\max} - \omega_{\min} \ll 2\pi/\tau,$$

and a small spectral window $[\tilde{\omega}_{\min}, \tilde{\omega}_{\max}]$ in the J-dimension. The latter could either coincide or be within the corresponding original Nyquist range (that is already small)

$$\tilde{\omega}_{\max} = -\tilde{\omega}_{\min} \leqslant \pi/\tilde{\tau}.$$

Consider a rectangular uniformly spaced frequency grid $(\varphi_j, \tilde{\varphi}_j)$ $(j = 1, \ldots, K_{\mathrm{win}})$ inside the chosen 2D window (see Fig. 3):

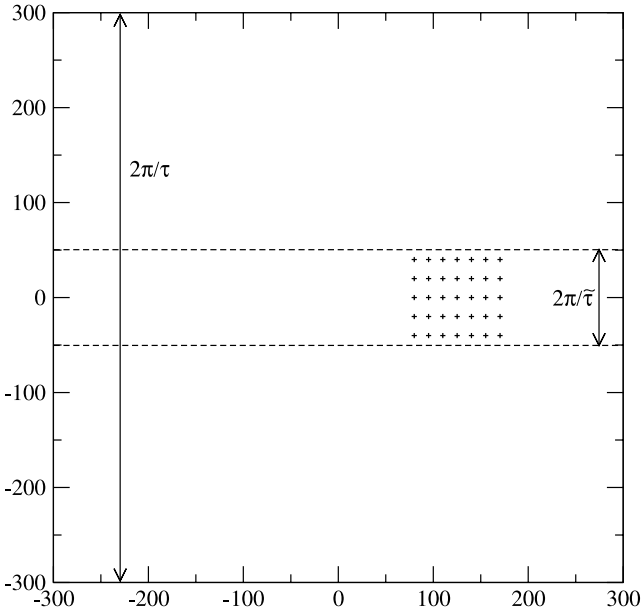

Fig. 3. An illustration of the Fourier basis functions for a particular frequency window. Note that although the spectral widths in both dimensions of the resampled signal are equal, the basis functions in the J dimension are entirely contained in the spectral region defined by the original experimental time step.

$$\omega_{\min} < \varphi_j < \omega_{\max}, \quad \tilde{\omega}_{\min} < \tilde{\varphi}_j < \tilde{\omega}_{\max}.$$

The corresponding grid spacings are not adjustable parameters and are set to

$$\Delta\varphi = \frac{4\pi}{N\tau}; \quad \Delta\tilde{\varphi} = \frac{4\pi}{M\tau}.$$

The 2D Fourier basis $\{\Psi_j\}$ $(j = 1, \ldots, K_{\mathrm{win}})$ is defined by

$$\Psi_j := \sum_{n=0}^{N/2-1} \sum_{m=0}^{M/2-1} (U/z_j)^n (\tilde{U}/\tilde{z}_j)^m \Phi \tag{19}$$

with $z_j := \mathrm{e}^{-\mathrm{i}\tau\varphi_j}$ and $\tilde{z}_j := \mathrm{e}^{-\mathrm{i}\tau\tilde{\varphi}_j}$. (Without any sacrifice we assumed both N and M to be even integers.)

By the bold characters $\mathbf{U}$, $\tilde{\mathbf{U}}$, and $\mathbf{S}$ we define the $K_{\mathrm{win}} \times K_{\mathrm{win}}$ matrix representations of, respectively, U, $\tilde{U}$, and I (the unit matrix) in the Fourier subspace:

$$\mathbf{S}_{jj'} := \Psi_j^{\mathrm{T}} \Psi_{j'}; \quad \mathbf{U}_{jj'} := \Psi_j^{\mathrm{T}} U \Psi_{j'}; \quad \tilde{\mathbf{U}}_{jj'} := \Psi_j^{\mathrm{T}} \tilde{U} \Psi_{j'}.$$

We will also need the two K_{win}-dimensional column vectors:

$$\mathbf{Y}_j := \Psi_j^{\mathrm{T}} \Phi; \quad \tilde{\mathbf{Y}}_j := \Psi_j^{\mathrm{T}} \tilde{U} \Phi.$$

The elements of $\mathbf{U}$, $\tilde{\mathbf{U}}$, $\mathbf{S}$, $\mathbf{Y}$, and $\tilde{\mathbf{Y}}$ can be expressed exclusively in terms of the data y_{nm} [6]. For completeness the relevant expressions are given in Appendix A. Using these expressions we can evaluate the spectra (17) and (18) in the Fourier subspace (see [5,12] for a derivation):

$$I_p(\omega) = z\tau \mathbf{Y}^{\mathrm{T}} \mathbf{R}^{-1} \tilde{\mathbf{Y}}, \tag{20}$$

$$I_p^{(2)}(\omega) = \tau^2 \mathbf{Y}^{\mathrm{T}} \mathbf{R}^{-1} \mathbf{S} \mathbf{R}^{-1} \mathbf{Y} \tag{21}$$

with the frequency dependent $K_{\mathrm{win}} \times K_{\mathrm{win}}$ matrix pencil $\mathbf{R} = z\tilde{\mathbf{U}} - \mathbf{U}$.

2.3.2. Regularization

For data sets satisfying Eq. (10) exactly the above two spectral estimation formulas converge very quickly to the exact spectra for frequencies ω inside the window, which define the Fourier basis (see Fig. 3). However, practically $\mathbf{R}$ may be very ill-conditioned and so these expressions implemented naively may contain artifacts or even give meaningless results. To remove the ill-conditioning we use the Singular Value Decomposition (SVD) of $\mathbf{R}$,

$$\mathbf{R} = \mathbf{V}^{\dagger} \mathbf{\Sigma} \mathbf{W} \tag{22}$$

with unitary matrices $\mathbf{V}$ and $\mathbf{W}$ and $\mathbf{\Sigma} = diag(\sigma_n)$, real and diagonal. Since we can now write $\mathbf{R}^{-1} = \mathbf{W}^{\dagger} \mathbf{\Sigma}^{-1} \mathbf{V}$, the problem then becomes that of regularizing the diagonal matrix $\mathbf{\Sigma}^{-1}$. Here the *truncated SVD* (i.e., setting $[\mathbf{\Sigma}_q^{-1}]_{nn} = 0$ for very small singular values σ_n below certain threshold) is not recommended. Instead, the more uniform regularization may be employed

$$\mathbf{\Sigma}_q^{-1} = (\mathbf{\Sigma}^2 + q\mathbf{I})^{-1} \mathbf{\Sigma}. \tag{23}$$

Even though the SVD based regularization is more computationally expensive than other methods [5], we prefer SVD because it allows us to generate the spectra, e.g., $I_p^{(2)}(\omega)$, at many values of q simultaneously for little additional cost.

The RRT expressions ((20) and (21)) for the spectral estimation of the 45° projections are new and constitute the main result of this paper. They are applicable to experimental data, which does not necessarily fit the model (1) exactly, even though it was assumed in the derivation. This will be demonstrated in the next section.

3. Experimental

As a test of our method we choose a simple representative carbohydrate: sucrose. The 1D proton spectrum is given in Fig. 4. In the proton dimension, 1024 points were collected, and 64 in the J dimension. The pulse sequence was a double spin-echo 2D-J experiment [8] shown in Fig. 5. Broadband inversion pulses, 60 μs in duration [18], were used to ensure that proper inversion was obtained. In addition, a long (1 s), low-power presaturation pulse was applied to the HOD resonance, to reduce the effect of the residual water on the spectrum.

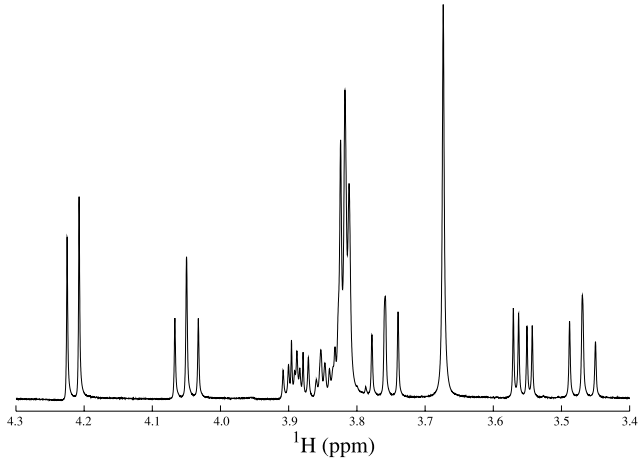

Fig. 4. Aliphatic region of the 1D proton spectrum of sucrose. The sample dissolved in D_2O, was run on a Varian Unity-INOVA 500 MHz spectrometer. In later figures we consider only the most crowded region of this spectrum, from 3.70 to 3.94 ppm. This was processed using 16 384 points.

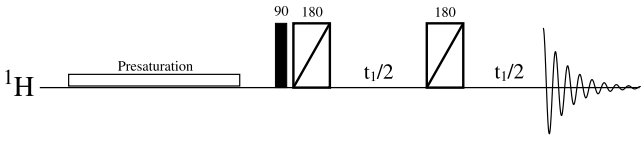

Fig. 5. Pulse sequence for the double spin-echo (DSE) 2D-J experiment. A standard 90° pulse and two broadband inversion 180° pulses 60 μs in duration were used. A slight delay was added to each t_1 increment in order to ensure that the resulting signal could be interpolated. In addition, a pre-saturation pulse was applied to the water signal in order to decrease its contribution to the rest of the spectrum.

4. Numerical results

The calculations using RRT were performed using only part (800×16) of the whole signal. We note here that truncation of the signal along the aquisition dimension (from $N = 1024$ to $N = 800$ in the present case) is beneficial for RRT as beyond certain time the tail of the FID does not provide any new information while it adds more noise. The number of basis functions in each window (K_{win}) was either 80 or 160. The regularization was applied using the SVD method to generate several spectra over a range of regularization parameters ($q = 0.0005$ to 0.05). The spectra did not differ much

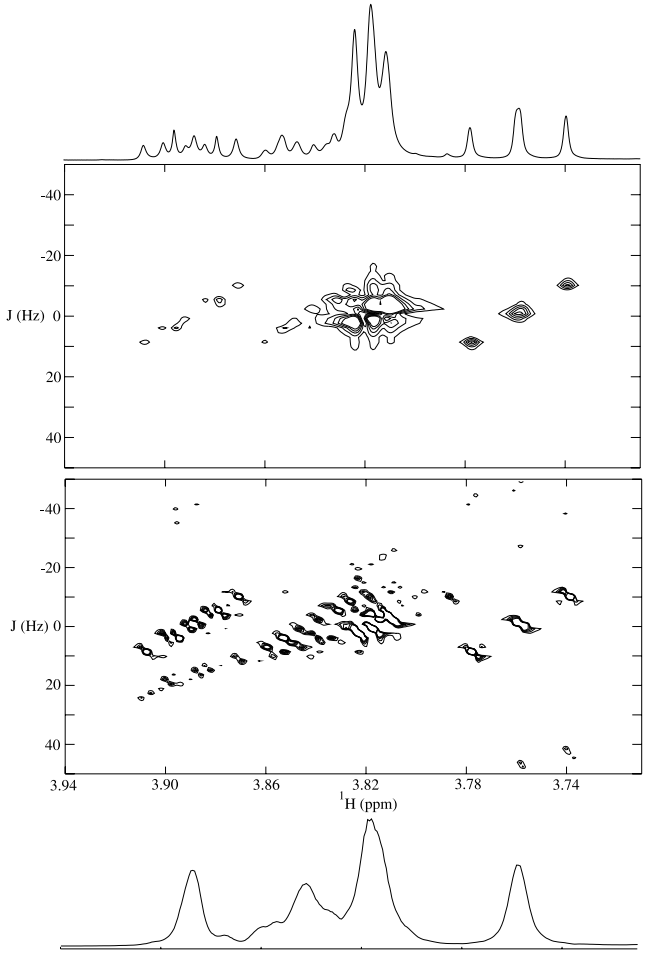

Fig. 6. The traditional method for processing 2D-J signals. The upper 2D spectrum is the normal cosine-apodized FT of the data. By constructing the 2D FT with sine-bell apodization (lower 2D spectrum), the projection along the 45° axis will yield better resolution (bottom trace). This trace should be absent of proton coupling. For comparison, the coupled 1D spectrum is presented at the top. These were all calculated using the full signal (1024×64).

over this large range, showing that the regularization is very robust. A small smoothing ($\Gamma = 0.1$ Hz) was also employed to reduce the effect of amplitude distortion by the pseudo-absorption formula.

For the FT, the best projections were obtained using a sine-bell weighting function [4]. While this procedure makes the 2D spectrum more difficult to analyze, it minimizes the artifacts discussed in the Introduction, and improves the resolution of the projection. The 2D FT of the data (with both cosine and sine-bell apodization) using 1024×64 points is given in Fig. 6 along with the regular 1D FT and the 45° projection of the 2D spectrum. The comparison of RRT with the FT using 16 points in the *J*-dimension is given in Fig. 7. Note that it is not possible to construct the sine-bell weighted spectrum for RRT, so the FT sine-bell spectrum is compared to the RRT pseudo-absorption spectrum [5]. It is evident that even with the *indirect* calculation of the 45° projection (i.e., via construction of the 2D spectrum) RRT offers resolution enhancement over the FT. However, even with this improvement the RRT 45° projection is not well resolved for this crowded spectral region.

Now we demonstrate that using the *direct* calculation of the 45° projection (i.e., without constructing the 2D spectrum) as described in this paper, a significant improvement can be achieved. The results for the most crowded region of the spectrum are shown in Fig. 8 and compared with the other methods. Even using the short signal (800×16) the projection computed directly by RRT gives resolution that is better than that obtained with the FT of the full signal (1024×64), and better than that from projection of the 2D RRT spectrum. All of the resonances for sucrose can now be resolved, including the two methylene resonances (~3.82 ppm) previously obscured. In addition, artifacts due to the experiment, such as strong coupling between resonances, can be identified. This direct method thus represents a vast improvement in processing *J*-resolved spectra.

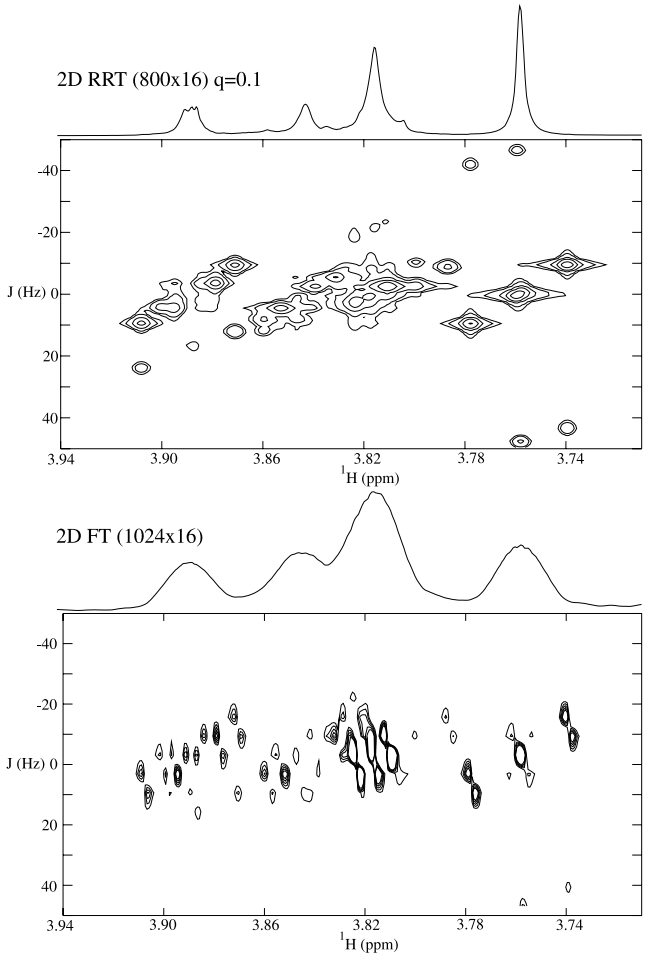

Fig. 7. A comparison of RRT with FT using only 16 points in the *J*-dimension. Both spectra have been calculated by constructing the 2D spectrum, and projecting along the 45° axis. While the FT spectrum has been apodized with a sine-bell function, the RRT spectrum has been constructed using the pseudo-absorption formula, and smoothed using gaussian convolution. The RRT result offers only a slight resolution enhancement, because the projection is not computed directly.

5. Conclusions

Due to the difficulty of spectral processing, *J*-resolved spectroscopy has been limited in its applications. This

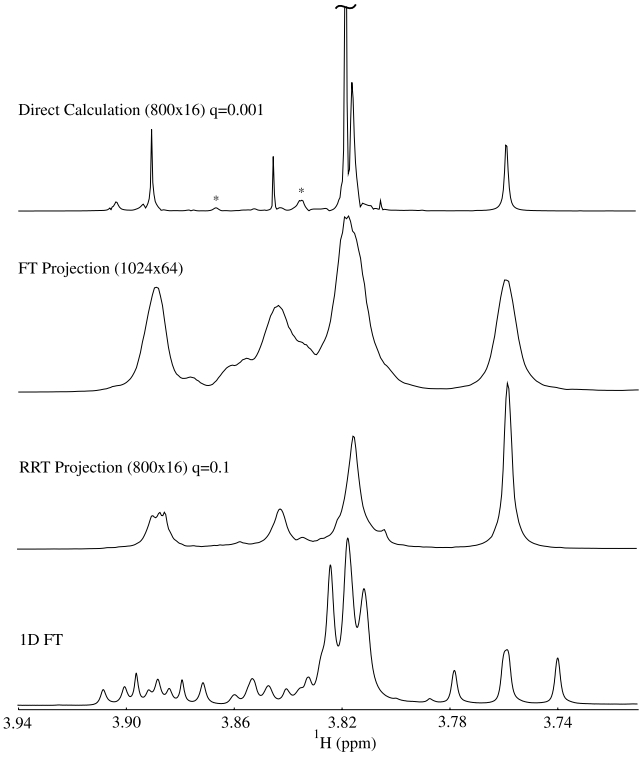

Fig. 8. Comparison of the 1D projected spectra for each method. For comparison the 1D FT is presented at the bottom. Finally the result from the method presented here is at the top. The direct calculation of the projection offers a considerable resolution advantage over the indirect approaches. Marked with an asterisk are peaks that are due to strong coupling.

has been due to the problem of obtaining a 45° projection of a magnitude 2D FT spectrum. Although an approach, based on FDM, of calculating directly the 45° projection was already proposed [15], it had certain drawbacks. Here we have revisited this approach. A tricky "scaling" problem was replaced by a simple signal resampling using interpolation, which produces a 2D time signal with the same spectral ranges in the two dimensions. The resampled data is then processed by RRT (or possibly with FDM) to directly generate a pseudo-absorption 45° projection. The resulting method yields excellent resolution of the uncoupled proton spectrum, even in the most crowded regions of the spectrum. Apart from the resolution enhancement, this method offers a significant experimental time savings in that not as much data are required for the calculation.

Finally, we point out that in the present work we have not made an effort to optimize the computer time for evaluating the expressions (20) and (21). Namely, computation of $I_p^{(2)}(\omega)$ at many values of ω requires multiple solution of the linear least squares problem

$$\mathbf{R}(\omega)\mathbf{X}(\omega) = \mathbf{Y} \tag{24}$$

with the ill-conditioned matrix-pencil $\mathbf{R}(\omega) = z\tilde{\mathbf{U}} - \mathbf{U}$ and $z := \mathrm{e}^{-\mathrm{i}\tau\omega}$. The approach based on RRT is robust, but may not be optimal in other respects. For example, solving the corresponding generalized eigenvalue problem (as in FDM) and then evaluating $\mathbf{X}(\omega)$ at many values of ω is much cheaper. Another significant computational saving may be achieved if Eq. 24 is solved iteratively by a conjugate gradient method with the initial guess for $\mathbf{X}(\omega)$ taken from the solution previously obtained for a nearby value of ω. These and other issues will be investigated in our forthcoming publications.

Acknowledgments

V.A.M. acknowledges the NSF support, Grant CHE-0108823. V.A.M. is an Alfred P. Sloan research fellow. A.J.S. was supported by the NSF Grant CHE-9900422.

Appendix A

The elements of the overlap matrix $\mathbf{S}$ are computed by

$$\mathbf{S}_{jj'} = \sigma \sum_{p=0,1} \frac{(-1)^p (z_j/z_{j'})^{pN/2}}{1 - z_j/z_{j'}} \tilde{\sigma} \sum_{\tilde{p}=0,1} \frac{(-1)^{\tilde{p}} (\tilde{z}_j/\tilde{z}_{j'})^{pM/2}}{1 - \tilde{z}_j/\tilde{z}_{j'}} \times \sum_{n=pN/2}^{(p+1)(N/2-1)} \sum_{m=\tilde{p}M/2}^{(\tilde{p}+1)(M/2-1)} z_j^{-n} \tilde{z}_j^{-m} y_{nm}, \tag{A.1}$$

where σ and $\tilde{\sigma}$ define the symmetrization operators over the corresponding pairs of variables:

$$\sigma g(z_j, z_{j'}) = g(z_j, z_{j'}) + g(z_{j'}, z_j),$$
$$\tilde{\sigma} g(\tilde{z}_j, \tilde{z}_{j'}) = g(\tilde{z}_j, \tilde{z}_{j'}) + g(\tilde{z}_{j'}, \tilde{z}_j).$$

For $z_j = z_{j'}$ and $\tilde{z}_j \neq \tilde{z}_{j'}$ we have

$$\mathbf{S}_{jj'} = \tilde{\sigma} \sum_{\tilde{p}=0,1} \tilde{z}_j \frac{(-1)^{\tilde{p}} (\tilde{z}_j/\tilde{z}_{j'})^{pM/2}}{1 - \tilde{z}_j/\tilde{z}_{j'}} \sum_{n=0}^{N-2} \sum_{m=\tilde{p}M/2}^{(\tilde{p}+1)(M/2-1)} \times z_j^{-n} \tilde{z}_j^{-m} y_{nm} (N/2 - |N/2 - n - 1|), \tag{A.2}$$

which can trivially be rewritten for the symmetric case of $z_j \neq z_{j'}$ and $\tilde{z}_j = \tilde{z}_{j'}$. For the case of both $z_j = z_{j'}$ and $\tilde{z}_j = \tilde{z}_{j'}$, i.e., the diagonal elements of the U-matrices, we have

$$\mathbf{S}_{jj} = \sum_{n=0}^{N-2} \sum_{m=0}^{M-2} z_j^{-n} \tilde{z}_j^{-m} y_{nm} (N/2 - |N/2 - n - 1|) \times (M/2 - |M/2 - m - 1|). \tag{A.3}$$

As can be seen the calculation of the $\mathbf{S}$ matrix elements require the knowledge of y_{nm} for $n = 0, \ldots, N-2$ and $m = 0, \ldots, M-2$. To compute the $\mathbf{U}$ and $\tilde{\mathbf{U}}$ matrices exactly the same equations ((A.1)–(A.3)) are applied to the shifted data arrays, respectively, $y_{n+1,m}$ and $y_{n,m+1}$ (see [12] for more details).

The matrix elements of the arrays $\mathbf{Y}$ and $\tilde{\mathbf{Y}}$ in terms of the signal are given by:

$$\mathbf{Y}_j = \sum_{n=0}^{N/2-1} \sum_{m=0}^{M/2-1} z_j^{-n} \tilde{z}_j^{-m} y_{nm},$$
$$\tilde{\mathbf{Y}}_j = \sum_{n=0}^{N/2-1} \sum_{m=0}^{M/2-1} z_j^{-n} \tilde{z}_j^{-m} y_{n,m+1}. \tag{A.4}$$

References

[1] W.P. Aue, J. Karhan, R.R. Ernst, Homonuclear broad-band decoupling and 2-dimensional *J*-resolved NMR spectroscopy, J. Chem. Phys. 64 (1976) 4226–4227.
[2] G. Bodenhausen, R. Freeman, R. Niedermeyer, D.L. Turner, Double Fourier transformation in high-resolution NMR, J. Magn. Reson. 26 (1977) 133–164.
[3] A. Bax, R. Freeman, Investigation of complex networks of spin–spin coupling by two-dimensional NMR, J. Magn. Reson. 44 (1981) 542–561.
[4] A. Demarco, K. Wüthrich, Digital filtering with a sinusoidal window function—alternative technique for resolution enhancement in FT NMR, J. Magn. Reson. 24 (1976) 201–204.
[5] J. Chen, A.J. Shaka, V.A. Mandelshtam, RRT: The regularized resolvent transform for high resolution spectral estimation, J. Magn. Reson. 147 (2000) 129–137.
[6] V.A. Mandelshtam, H.S. Taylor, Multidimensional harmonic inversion by filter-diagonalization, J. Chem. Phys. 108 (1998) 9970–9977.
[7] M.R. Wall, T. Dieckmann, J. Feigon, D. Neuhauser, Two-dimensional filter-diagonalization: spectral inversion of 2D NMR time-correlation signals including degeneracies, Chem. Phys. Lett. 291 (1998) 465–470.
[8] V.A. Mandelshtam, H.S. Taylor, A.J. Shaka, Application of the filter diagonalization method to one- and two-dimensional NMR spectra, J. Magn. Reson. 133 (1998) 304–312.

[9] V.A. Mandelshtam, N.D. Taylor, H. Hu, M. Smith, A.J. Shaka, Highly resolved double absorption 2D NMR spectra from complex severely truncated 2D phase modulated signals by filter-diagonalization-averaging method, Chem. Phys. Lett. 305 (1999) 209–216.
[10] V.A. Mandelshtam, The multidimensional filter diagonalization method. I. Theory and numerical implementation, J. Magn. Reson. 144 (2000) 343–356.
[11] J. Chen, V.A. Mandelshtam, A.J. Shaka, Regularization of the filter diagonalization method: FDM2k, J. Magn. Reson. 146 (2000) 363–368.
[12] V.A. Mandelshtam, FDM: the filter diagonalization method for data processing in NMR experiments, Prog. Nucl. Magn. Reson. Spectrosc. 38 (2001) 159–196.
[13] A. Neumaier, Solving ill-conditioned and singular linear systems: a tutorial on regularization, SIAM Rev. 40 (1998) 636–666.
[14] J. Demmel, B. Kågström, The generalized Schur decomposition of an arbitrary pencil A-zB: robust software with error bounds and applications. Part I: theory and algorithms, ACM T. Math. Software 19 (1993) 160–174.
[15] V.A. Mandelshtam, Q.N. Van, A.J. Shaka, Obtaining proton chemical shifts and multiplets from several 1D NMR signals, J. Am. Chem. Soc. 120 (1998) 12161–12162.
[16] A.A. De Angelis, H. Hu, V.A. Mandelshtam, A.J. Shaka, The multidimensional filter diagonalization method. II. Applications to 2D, 3D and 4D NMR experiments, J. Magn. Reson. 144 (2000) 357–366.
[17] C. De Boor, A Practical Guide to Splines, Springer, New York, 1978.
[18] M.A. Smith, H. Hu, A.J. Shaka, Improved broadband inversion performance for NMR in liquids, J. Magn. Reson. 151 (2001) 269–283.